Supplement of Atmos. Chem. Phys., 22, 4237–4252, 2022
https://doi.org/10.5194/acp-22-4237-2022-supplement

Atmospheric Chemistry and Physics
Open Access

Supplement of

Formation of organic sulfur compounds through SO_2-initiated photochemistry of PAHs and dimethylsulfoxide at the air-water interface

Haoyu Jiang et al.

Correspondence to: Sasho Gligorovski (gligorovski@gig.ac.cn)

Section S1. Description of MI-SPI-TOF-MS

Section S2. Description of FT-ICR-MS

Section S3. Analysis of FT-ICR-MS aqueous phase products based on DBE *vs* carbon number iso-abundance plot

Section S4. Reaction mechanism of the aqueous phase product compounds

Section S5. Tables, Figures and Scheme

Number of Pages: 47

Number of Tables: 6

Number of Figures: 16

Number of Schemes: 1

Section 1. MI-SPI-TOF-MS

Briefly, a polydimethylsiloxane (PDMS, thickness 0.002 inch, Technical Products Inc, USA) membrane was used in the injector of the TOF-MS.[53] The ionization of the compounds (SPI) was performed by vacuum ultraviolet (VUV) light emitted by a deuterium (D_2) lamp (Hamamatsu, Japan): This is a soft ionization technique characterized by high molecular ion yield and low degree of fragmentation.[60-62] The limit of detection (LOD) of TOF-MS is around 1 ppb for most trace gases, and the time resolution of SPI-MS was set to 5 s.

The raw data were analyzed with commercial software (SPI-MS 3000 V1.0.1.2.0, Guangzhou Hexin Instrument Co., Ltd., China), where the selected Gauss peaks above a preset threshold are smoothed with a given average number.

Section 2. FT-ICR-MS

A solariX XR FT-ICR-MS instrument (Bruker Daltonik GmbH, Bremen, Germany) equipped with a refrigerated, 9.4 T actively shielded superconducting magnet (Bruker Biospin, Wissembourg, France) and a Paracell analyzer cell was used to detect the formation of products in the bulk aqueous phase.[53] Sample ionization was performed in the negative ion mode using an electrospray ionization (ESI) ion source (Bruker Daltonik GmbH, Bremen, Germany). The detection mass range was set at 150-1,000 m/z. Ion accumulation time was set at 0.65 s. Details of this instrument setting, calibration and data processing were described in previous publications.[63, 64]

Section 3. Analysis of FT-ICR-MS Aqueous Phase Products Based on DBE *vs* Carbon Number Iso-Abundance Plot

The iso-abundance plots of DBE versus carbon numbers for the detected CHO and CHOS formulae formed upon light-induced SO_2 oxidation of DMSO and PAHs/DMSO are presented in Figure S7-8. The CHO and CHOS with the same DBE values but different carbon numbers are considered as homologs differing from each other by a repeating mass increment.[1]

The CHO and CHOS products distributions formed by SO_2 photo-oxidation of PAHs/DMSO were different than those formed upon SO_2 photo-oxidation of DMSO, whereas the former had a regular and convergent distribution, while the latter distribution of products was more scattered. The DBE values are smaller than six for most of the CHO compounds formed upon SO_2 photo-oxidation of DMSO, whereas only 9 out of 16 CHOS products had low DBE values ranging from 0 to 6. Those OS products with relatively high DBE values over eleven usually along with carbon numbers from 27 to 42, indicates the probable formation of unsaturated long-chain aliphatic-like OSs compounds.

Considering the light-induced heterogeneous reaction of SO_2 with PAHs/DMSO (Figure S7), generally, the depicted average properties in terms of DBE and carbon number of numerous products for the PYR/DMSO almost contain the average properties of products for FLA/DMSO and PHE/DMSO. Both of the CHO and CHOS products formed in liquid phase could be divided into two clusters. Most of the CHO products, especially those emerged by light-induced heterogeneous reaction of SO_2 with

PYR/DMSO, exhibited DBE values in the range of 8-14 and 2-7, with 10-19 carbon atoms and 1-9 oxygen atoms, which would probably be the hydroxyl or carboxyl compounds. [2, 3] The products formed by light-induced heterogeneous reaction of SO_2 with PHE/DMSO had lower DBE than those produced by light-induced heterogeneous reaction of SO_2 with FLA/DMSO. The DBE values between 1 and 3 for products formed by light-induced heterogeneous reaction of SO_2 with PHE/DMSO and 6-7 for products formed by light-induced heterogeneous reaction of SO_2 with FLA/DMSO exhibited a relatively long carbon chain compared with those corresponding in the other cluster, which is 23-32 and 21-32, respectively, implying that these compounds were most likely the photodegradation products of the initial reactants. There is no significant difference of O atom in these two clusters.

Similarly, the majority of CHOS exhibited DBE values in the range of 8-13 and 1-5, with 13 to 16 and 6-17 carbon atoms, and 4 to 10 oxygen atoms. Almost all the CHOS products were with only one sulfur atom. The limited carbon number indicated these CHOS products were still inclined to maintain an original aromatic structure from reactants.

Section 4. Reaction Mechanism of the Aqueous Phase Product Compounds

The heterogeneous reaction between SO_2 and unsaturated fatty acid and long-chain alkenes has been reported to take place and leads efficiently to the formation of OSs.[4, 5] In our study, OS products formed by light-induced SO_2 oxidation of PAHs may also follow similar reaction mechanism. The key step is the formation of cyclic organosulfites and linear OS products by the isomerization of a double bond (C=C) *via* ene-reactions between SO_2 and the double bond. The first step includes evolvement of diaradical OS intermediates via two routes, i.e. the direct interaction of SO_2 with the C=C leading to π complexes, and a four-membered ring formation through a [2+2] cycloaddition. After the SO_2 addition to the C=C double bond, oxidation reactions would be triggered, undergoing radical-initiated H-abstraction, OH radical production and chain fragmentation which ultimately leads to the formation of stable cyclic organosulfites by the intramolecular recombination of radicals. [4, 5] As expected, OS compounds with sulfoxide group such as $C_{16}H_{10}O_3S$ (1, 3), and $C_{14}H_{10}O_3S$ (2) were generated by $^3SO_2$* oxidation of ^{3}PYR*, ^{3}FLA*, and ^{3}PHE*. Meanwhile, $C_{16}H_{12}O_3S$ (4, 6) and $C_{14}H_{12}O_3S$ (5) could be also generated with the phenyl ring open at the position of 10a, 1 and 5a, 5 of PYR, 10a, 1 and 8a, 9 of PHE, and 10a, a and 3a, a of FLA. All these initial products would be oxidized into sulfones, such as $C_{16}H_{10}O_4S$ (7, 9) and $C_{14}H_{10}O_4S$ (8), then followed by subsequent further oxidation. With the attack of oxygen and radicals, a five-membered ring was allowed to open, yielding the formation of aromatic sulfates including 1-pyrenylsulfate ($C_{16}H_{10}O_4S$) (10), 4-pyrenylsulfate ($C_{16}H_{10}O_4S$) (11), 3-phenanthrol sulfate ($C_{14}H_{10}O_4S$) (12), 9-

phenanthrol sulfate ($C_{14}H_{10}O_4S$) (13), 8-fluoranthenyl sulfate ($C_{16}H_{10}O_4S$) (14), and 1-fluoranthenyl sulfate ($C_{16}H_{10}O_4S$) (15). A further degradation initiated by triggering phenyl ring open, smaller degradation products with aromatic ring structures could be generated.

Section 5. Tables, Figures and Scheme

Table S1: Calculated Gibbs free energies for all molecules employed in the derivation of gas-phase reaction Gibbs energies in transformation process initiated by ^{3}PAHs* with SO_2, arranged in the order of increasing molecular mass.

Chemical Formula or Name	G_m^{Θ}/Hartree
·CH_3	-39.81
·OH	-75.74
H_2O	-76.42
CH_2O	-114.49
·OCH_3	-115.03
·CH_2OH	-115.04
O_2	-150.28
CH_3OH	-115.69
CO_2	-188.61
·$OOCH_3$	-190.19
SO_2	-548.64
($^3\Sigma$)SO_2	-548.54
HOSO·	-549.21
$S(=O)(CH_3)_2$	-553.14
SO_3	-623.84
$CH_3S(=O)OH$	-589.09
$S(=O)_2(CH_3)_2$	-628.37
$CH_3S(=O)_2OH$	-664.33
H_2SO_4	-700.28
$CH_3S(=O)_2OCH_3$	-703.60
$HOS(=O)OOCH_3$	-739.45
$CH_2(OH)S(=O)_2OH$	-739.55
CH_2=CH($OS(=O)_2OH$)	-777.63
cyclo-(CH=$CHOS(=O)_2O$)	-776.43
$CH_3CH_2(OS(=O)_2OH)$	-778.84
$CH_2(OH)CH_2S(=O)_2OH$	-778.83
$S(=O)_2(CH2OH)_2$	-778.81
Z-CH_3CH=CH($OS(=O)_2OH$)	-816.92
$CH_3S(=O)_2OCH_2CH_2OH$	-818.11

$S(=O)_2(COOH)_2$	-926.92
$CH_3S(=O)_2OCH_2COOH$	-892.18
C_5H_4-1-($OS(=O)_2OH$)	-893.09
C_6H_4-1,2-(cyclo-$OS(=O)_2O$)	-930.04
C_6H_5-1-($OS(=O)_2OH$)	-931.24
$S(=O)_2(OCOOH)_2$	-1077.42
$C_{10}H_6$-2,3-(cyclo-OS(=O)O)	-1008.41
$C_{10}H_7$-2-(OS(=O)OH)	-1009.60
C_9H_7-1-($OS(=O)_2OH$)	-1046.70
$C_{10}H_6$-2,3-(cyclo-$OS(=O)_2O$)	-1083.63
$C_{10}H_7$-2-($OS(=O)_2OH$)	-1084.83

Table S2: Calculated Gibbs free energies for all molecules employed in the derivation of aqueous-phase reaction Gibbs energies in transformation process initiated by ^{3}FLA*, arranged in the order of increasing molecular mass.

Chemical Formula or Name	G_m^{Θ}/Hartree
Fluoranthene	-615.54
($^3\Sigma$)Fluoranthene	-615.48
$C_{16}H_8$-(8H,9H)-8,9-(cyclo-OS(=O)O)	-1239.38
$C_{16}H_8$-(1H,2H)-1,2-(cyclo-OS(=O)O)	-1239.39
E-$C_{12}H_6$-1-(CH=CHCH=CH_2)-2-(OS(=O)OH)	-1240.54
E-$C_{13}H_7$-1-(OS(=O)OH)-9-(=CHCH=CH_2)	-1240.56
$C_{16}H_8$-(8H,9H)-8,9-(cyclo-OS(=O)$_2$O)	-1314.61
$C_{16}H_9$-8-(OS(=O)$_2$OH)	-1314.66
$C_{16}H_8$-(1H,2H)-1,2-(cyclo-OS(=O)$_2$O)	-1314.62
E-$C_{12}H_6$-1-(CH=CHCH=CH_2)-2-(OS(=O)$_2$OH)	-1315.78
$C_{16}H_9$-1-(OS(=O)$_2$OH)	-1314.66
E-$C_{13}H_7$-1-(OS(=O)$_2$OH)-9-(=CHCH=CH_2)	-1315.80
$C_{16}H_8$-8-(OS(=O)$_2$OH)-9-OH	-1389.89
$C_{16}H_9$-1-(OS(=O)$_2$OH)-2-OH	-1389.89
E-$C_{12}H_6$-1-(CH=CHCOOH)-2-(OS(=O)$_2$OH)	-1427.19
E-$C_{13}H_7$-1-(OS(=O)$_2$OH)-9-(=CHCHCOOH)	-1426.00
(1E,2E)-$C_{12}H_6$-1-(=CHC(=O)OS(=O)$_2$OH)-2-(=CHCOOH)	-1540.33
E-$C_{13}H_7$-1-(=CHCOOH)-9-(C(=O)OS(=O)$_2$OH)	-1540.32

Table S3: Calculated Gibbs free energies for all molecules employed in the derivation of aqueous-phase reaction Gibbs energies in transformation process initiated by ^{3}PHE* and ^{3}PYR*, arranged in the order of increasing molecular mass.

Chemical Formula or Name	G_m^{Θ}/Hartree
Phenathrene	-539.34
($^3\Sigma$)Phenathrene	-539.26
Pyrene	-615.56
($^3\Sigma$)Pyrene	-615.48
$C_{14}H_8$-(2H,3H)-2,3-(cyclo-OS(=O)O)	-1163.17
$C_{14}H_8$-(9H,10H)-9,10-(cyclo-OS(=O)O)	-1163.20
E-$C_{10}H_6$-1-(CH=CHCH=CH_2)-2-(OS(=O)OH)	-1164.35
$C_{12}H_8$-2-(CH=CH_2)-2'-OS(=O)OH	-1164.36
$C_{14}H_8$-(2H,3H)-2,3-(cyclo-OS(=O)$_2$O)	-1238.40
$C_{14}H_9$-3-(OS(=O)$_2$OH)	-1238.46
$C_{14}H_8$-(9H,10H)-9,10-(cyclo-OS(=O)$_2$O)	-1238.44
$C_{14}H_9$-9-(OS(=O)$_2$OH)	-1238.46
E-$C_{10}H_6$-1-(CH=CHCH=CH_2)-2-(OS(=O)$_2$OH)	-1239.59
$C_{12}H_8$-2-(CH=CH_2)-2'-OS(=O)$_2$OH	-1239.60
$C_{16}H_8$-(2H,3H)-2,3-(cyclo-OS(=O)O)	-1239.38
$C_{16}H_8$-(4H,5H)-4,5-(cyclo-OS(=O)O)	-1239.43
E-$C_{13}H_7$-1H-1-(=CHCH=CH_2)-9-(OS(=O)OH)	-1240.56
$C_{14}H_8$-4-(OS(=O)OH)-5-(CH=CH_2)	-1240.56
$C_{14}H_8$-2-OH-3-(OS(=O)$_2$OH)	-1313.69
$C_{14}H_8$-9-OH-10-(OS(=O)$_2$OH)	-1313.68
E-$C_{10}H_6$-1-(CH=CHCOOH)-2-(OS(=O)$_2$OH)	-1350.81
$C_{12}H_8$-2-COOH-2'-OS(=O)$_2$OH	-1350.82
$C_{16}H_8$-(2H,3H)-2,3-(cyclo-OS(=O)$_2$O)	-1314.61
$C_{16}H_9$-2-(OS(=O)$_2$OH)	-1314.66
$C_{16}H_8$-(4H,5H)-4,5-(cyclo-OS(=O)$_2$O)	-1314.66
$C_{16}H_9$-4-(OS(=O)$_2$OH)	-1314.68
E-$C_{13}H_7$-1H-1-(=CHCH=CH_2)-9-(OS(=O)$_2$OH)	-1315.79
$C_{14}H_8$-4-(OS(=O)$_2$OH)-5-(CH=CH_2)	-1315.80
$C_{16}H_8$-1-OH-2-(OS(=O)$_2$OH)	-1389.91
$C_{16}H_8$-2-(OS(=O)$_2$OH)-5-OH	-1389.90
E-$C_{13}H_7$-1H-1-(=CHCOOH)-9-(OS(=O)$_2$OH)	-1427.01

$C_{14}H_8$-4-(OS(=O)$_2$OH)-5-COOH	-1427.03
(1Z,2E)-$C_{10}H_6$-(1H,2H)-1-(=CHC(=O)OS(=O)$_2$OH)-2-(=CHCOOH)	-1464.31
$C_{12}H_8$-2-COOH-2'-C(=O)OS(=O)$_2$OH	-1464.16
$C_{14}H_8$-4-(C(=O)OS(=O)$_2$OH)-5-COOH	-1540.37
E-$C_{13}H_7$-1H-1-(=CHC(=O)OS(=O)$_2$OH)-9-COOH	-1540.35

146

147

Table S4: All detected m/z signals upon SO_2 oxidation of DMSO and a mixture of PAHs/DMSO under all conditional experiments.

m/z signals			
Pyrene	Fluoranthene	Phenanthrene	DMSO
42	32	46	32
46	42	48	34
48	46	50	42
50	48	58	46
58	50	62	48
60	56	64	50
62	58	66	56
64	62	72	58
66	64	74	60
72	70	76	62
74	72	78	64
76	74	80	66
78	76	82	70
80	78	88	72
82	80	90	74
88	82	92	76
90	84	94	78
92	88	96	80
94	86	100	82
96	90	102	84
100	92	106	88
102	94	108	90
106	96	110	92
108	98	112	94
110	100	122	96
112	102	124	98
118	104	126	100
120	106	128	102
122	108	136	104
124	110	138	106
126	112	140	108
136	118	142	110
138	120	154	112
140	122	156	114
154	126	158	116
156	128	166	118
158	134	170	120
166	136	178	122

170	142	180	124
178	166	182	126
180	178	184	128
	180	192	136
	182	194	138
		196	140
		204	142
		206	150
		208	152
		210	154
		222	156
			158
			160
			166
			168
			170
			178
			180
			182
			202
			204
			206
			208
			210

Table S5: Tentative gaseous organic unsaturated multifunctional molecules and sulfur compounds identification of detected *m/z* upon heterogeneous SO_2 oxidation of PAHs/DMSO dissolved in water.

Sample	m/z	PAHs/DMSO		DMSO	
		Tentative CHO	Tentative OS	Tentative CHO	Tentative OS
DMSO	34			H_2O_2	H_2S
	114			$C_5H_6O_3$	C_5H_6OS
				$C_6H_{10}O_2$	
				$C_7H_{14}O$	
	116			$C_4H_4O_4$	C_5H_8OS
				$C_5H_8O_3$	
	150			$C_8H_6O_3$	$C_4H_6O_4S$
				$C_9H_{10}O_2$	$C_5H_{10}OS_2$
				$C_{10}H_{14}O$	$C_5H_{10}O_3S$
					$C_6H_{14}O_2S$
	152			$C_8H_8O_3$	$C_4H_8O_2S_2$
				$C_9H_{12}O_2$	**$C_4H_8O_4S$**
	160			$C_6H_8O_5$	$C_7H_{12}O_2S$
				$C_7H_{12}O_4$	$C_8H_{16}OS$
				$C_8H_{16}O_3$	
	168			$C_8H_8O_4$	$C_8H_8O_2S$

				$C_{12}H_8O$	**$C_5H_{12}O_4S$**
				$C_9H_{12}O_3$	$C_5H_{12}O_2S_2$
					$C_9H_{12}OS$
	202			$C_{12}H_{10}O_3$	**$C_7H_6O_5S$**
				$C_9H_{14}O_5$	**$C_8H_{10}O_4S$**
				$C_{13}H_{14}O_2$	$C_8H_{10}O_2S_2$
				$C_{14}H_{18}O$	$C_9H_{14}OS_2$
				$C_{11}H_{22}O_3$	$C_{10}H_{18}O_2S$
					$C_{11}H_{22}OS$
FLA/DMSO	86	$C_3H_2O_3$	C_4H_6S		
		$C_4H_6O_2$	$C_6H_{14}OS$		
		$C_5H_{10}O$			
	134	$C_4H_6O_5$	$C_5H_{10}O_2S$		
		$C_8H_6O_2$	$C_6H_{14}OS$		
		$C_5H_{10}O_4$			
		$C_9H_{10}O$			
PHE/DMSO	**184**	$C_8H_8O_5$	**$C_5H_{12}O_5S$**		
		$C_{12}H_8O_2$	**$C_4H_8O_6S$**		
		$C_9H_{12}O_4$			
		$C_{11}H_{20}O_2$			
		$C_{13}H_{12}O$			

	192	$C_9H_4O_5$	**$C_6H_8O_5S$**	
		$C_{10}H_8O_4$	**$C_7H_{12}O_4S$**	
		$C_{14}H_8O$		
		$C_{11}H_{12}O_3$		
		$C_{12}H_{16}O_2$		
	194	$C_{10}H_{10}O_4$	**$C_5H_6O_6S$**	
		$C_{14}H_{10}O$	**$C_6H_{10}O_5S$**	
		$C_{11}H_{14}O_3$	**$C_7H_{14}O_4S$**	
		$C_{12}H_{18}O_2$		
	196	$C_9H_8O_5$	**$C_5H_8O_6S$**	
		$C_{13}H_8O_2$	**$C_6H_{12}O_5S$**	
		$C_{10}H_{12}O_4$	**$C_7H_{16}O_4S$**	
		$C_{14}H_{12}O$		
		$C_{11}H_{16}O_3$		
		$C_{12}H_{20}O_2$		
	222	$C_{11}H_{10}O_5$	**$C_5H_2O_8S$**	
		$C_{15}H_{10}O_2$	**$C_7H_{10}O_6S$**	
		$C_{12}H_{14}O_4$	**$C_8H_{14}O_5S$**	
		$C_{16}H_{14}O$	**$C_9H_{18}O_4S$**	
FLA/DMSO and DMSO	32	CH_4O		
	56	C_3H_4O	C_2S	C_2S
	70	C_4H_6O	C_3H_2S	C_3H_2S

	84	$C_4H_4O_2$	C_4H_4S	C_4H_4S
		C_5H_8O		
	104	$C_3H_4O_4$	C_4H_8OS	C_4H_8OS
		$C_4H_8O_3$		
PYR/DMSO and DMSO	60	$C_2H_4O_2$	C_2H_4S	C_2H_4S
PHE/DMSO and DMSO	**98**	$C_5H_6O_2$	**H_2O_4S**	**H_2O_4S**
		$C_6H_{10}O$	**C_5H_6S**	**C_5H_6S**
	182	$C_9H_{10}O_4$	**$C_4H_6O_6S$**	**$C_4H_6O_6S$**
		$C_{10}H_{14}O_3$	**$C_5H_{10}O_5S$**	**$C_5H_{10}O_5S$**
		$C_{11}H_{18}O_2$	**$C_6H_{14}O_4S$**	**$C_6H_{14}O_4S$**
	204	$C_{12}H_{12}O_3$	$C_{10}H_{20}O_2S$	$C_{10}H_{20}O_2S$
		$C_{13}H_{16}O_2$	**$C_7H_8O_5S$**	**$C_7H_8O_5S$**
	206	$C_{10}H_6O_5$	**$C_7H_{10}O_5S$**	**$C_7H_{10}O_5S$**
		$C_{11}H_{10}O_4$	**$C_8H_{14}O_4S$**	**$C_8H_{14}O_4S$**
		$C_{12}H_{14}O_3$	$C_8H_{14}O_2S_2$	$C_8H_{14}O_2S_2$
		$C_{13}H_{18}O_2$	$C_9H_{18}O_3S$	$C_9H_{18}O_3S$
		$C_{14}H_{22}O$	$C_{10}H_{22}O_2S$	$C_{10}H_{22}O_2S$
	208	$C_{10}H_8O_5$	**$C_6H_8O_6S$**	**$C_6H_8O_6S$**
		$C_{14}H_8O_2$	**$C_7H_{12}O_5S$**	**$C_7H_{12}O_5S$**
		$C_{11}H_{12}O_4$	**$C_8H_{16}O_4S$**	**$C_8H_{16}O_4S$**
		$C_{15}H_{12}O$	$C_8H_{16}O_2S_2$	$C_8H_{16}O_2S_2$
		$C_{12}H_{16}O_3$		

		$C_{13}H_{20}O_2$		
	210	$C_9H_6O_6$	**$C_6H_{10}O_6S$**	**$C_6H_{10}O_6S$**
		$C_6H_{10}O_8$	**$C_7H_{14}O_5S$**	**$C_7H_{14}O_5S$**
		$C_{10}H_{10}O_5$	**$C_8H_{18}O_4S$**	**$C_8H_{18}O_4S$**
		$C_{14}H_{10}O_2$		
		$C_{11}H_{14}O_4$		
		$C_{15}H_{14}O$		
		$C_{12}H_{18}O_3$		
		$C_{13}H_{22}O_2$		
PYR/DMSO, FLA/DMSO and DMSO	42	$C_2H_2O\cdot$	C_3H_6	C_3H_6
	118	$C_4H_6O_4$	$C_4H_6O_2S$	$C_4H_6O_2S$
		C_8H_6O	$C_5H_{10}OS$	$C_5H_{10}OS$
		$C_5H_{10}O_3$		
	120	$C_3H_4O_5$	$C_4H_8O_2S$	$C_4H_8O_2S$
		C_8H_8O	$C_5H_{12}OS$	$C_5H_{12}OS$
	122	$C_7H_6O_2$	$C_4H_{10}O2S$	$C_4H_{10}O_2S$
		$C_7H_8O_2$		
		$C_8H_{12}O$		
		$C_7H_6O_2$		
	138	$C_7H_6O_3$	$C_4H_{10}O_3S$	$C_4H_{10}O_3S$
		$C_6H_4O_4$		
		$C_7H_8O_3$		

		$C_8H_{12}O_2$		
	140	$C_7H_8O_3$	C_7H_8OS	**$C_3H_8O_4S$**
		$C_8H_{12}O_2$	$C_6H_4O_2S$	
FLA/DMSO, PHE/DMSO and DMSO	128	$C_{10}H_8$	$C_2H_8O_4S$	$C_2H_8O_4S$
			$C_5H_4O_2S$	$C_5H_4O_2S$
			C_6H_8OS	C_6H_8OS
	142	$C_6H_6O_4$	$C_6H_6O_2S$	$C_6H_6O_2S$
		$C_9H_6O_2$	$C_7H_{10}OS$	$C_7H_{10}OS$
PYR/DMSO, PHE/DMSO and DMSO	66	C_5H_6	H_2O2S	H_2O2S
	124	$C_7H_8O_2$	**$C_3H_8O_3S$ (EMS)**	**$C_3H_8O_3S$ (EMS)**
		$C_8H_{12}O$	**$C_2H_4O_4S$**	**$C_2H_4O_4S$**
	154	$C_7H_6O_4$	**$C_4H_{10}O_4S$**	**$C_4H_{10}O_4S$**
		$C_8H_{10}O_3$	**$C_3H_6O_5S$**	**$C_3H_6O_5S$**
		$C_{10}H_{18}O$	$C_8H_{10}OS$	C_8H_10OS
	156	$C_{11}H_8O$	**$C_2H_4O_6S$**	**$C_2H_4O_6S$**
		$C_7H_8O_4$	$C_7H_8O_2S$	$C_7H_8O_2S$
			$C_8H_{12}OS$	$C_8H_{12}OS$
	158	$C_{10}H_6O_2$	$C_6H_6OS_2$	$C_6H_6OS_2$
		$C_7H_{10}O_4$		$C_7H_{10}O_2S$
		$C_{11}H_{10}O$	$C_8H_{14}OS$	$C_8H_{14}OS$
	170	$C_8H_{14}O_3$	**$C_3H_6O_6S$**	**$C_3H_6O_6S$**
		$C_7H_6O_5$	**$C_4H_{10}O_5S$**	**$C_4H_{10}O_5S$**
		$C_{12}H_{10}O$	$C_7H_6O_3S$	$C_7H_6O_3S$

		$C_{10}H_{18}O_2$	$C_8H_{10}O_2S$		$C_8H_{10}O_2S$
PAHs/DMSO and DMSO	46	CH_2O_2	CH_2S		CH_2S
	48	CH_4O_2	OS		OS
	50	CH_2O	H_2OS		H_2OS
	58	$C_2H_2O_2$	C_2H_2S		C_2H_2S
		C_3H_6O			
	62	CH_2O_3	CH_2OS		CH_2OS
	64	CH_4O_3	CH_4OS		CH_4OS
	72	$C_3H_4O_2$	C_3H_4S		C_3H_4S
		C_4H_8O			
	74	$C_2H_2O_3$	C_2H_2OS		C_2H_2OS
		$C_3H_6O_2$			
	76	$C_2H_4O_3$	C_2H_4OS		C_2H_4OS
		$C_3H_8O_2$			
	78	C_6H_6	C_2H_6OS		C_2H_6OS
	80	C_5H_4O	**CH_4O_2S (MSIA)**		**CH_4O_2S (MSIA)**
	88	$C_3H_4O_3$	C_4H_8S		C_4H_8S
		$C_4H_8O_2$			
		$C_5H_{12}O$			
	90	$C_2H_2O_4$	C_3H_6OS		C_3H_6OS
		$C_3H_6O_3$			
		$C_4H_{10}O_2$			

92	C_6H_4O	$C_2H_4O_2S$		$C_2H_4O_2S$
	$C_2H_4O_4$	C_3H_8OS		C_3H_8OS
	$C_3H_8O_3$			
94	C_6H_6O	**$C_2H_6O_2S$ (MSM)**		**$C_2H_6O_2S$ (MSM)**
96	C_6H_8O	**CH_4O_3S (MSA)**		**CH_4O_3S (MSA)**
	$C_5H_4O_2$			
	$C_5H_6O_2$			
100	$C_4H_4O_3$	C_4H_4OS		C_4H_4OS
	$C_5H_8O_2$			
	$C_6H_{12}O$			
102	$C_4H_6O_3$	C_4H_6OS		C_4H_6OS
	$C_5H_{10}O_2$			
106	C_7H_6O	$C_3H_8O_2S$		$C_3H_8O_2S$
		$C_2H_4O_3S$		$C_2H_4O_3S$
108	$C_6H_4O_2$	$C_3H_8O_2S$		$C_3H_8O_2S$
110	$C_6H_6O_2$	$C_2H_6O_3S$		$C_2H_6O_3S$
112	$C_6H_8O_2$	**CH_4O_4S (MSAOH)**		**CH_4O_4S (MSAOH)**
	$C_7H_{12}O$	C_5H_4OS		C_5H_4OS
126	$C_6H_6O_3$	**$C_2H_6O_4S$ (ESAOH)**		**$C_2H_6O_4S$ (ESAOH)**
		C_6H_6OS		C_6H_6OS
136	$C_8H_8O_2$	$C_4H_8O_3S$		$C_4H_8O_3S$
	$C_5H_{12}O_4$	$C_5H_{12}O_2S$		$C_5H_{12}O_2S$

	$C_9H_{12}O$		
166	$C_8H_6O_4$	**$C_4H_6O_5S$**	**$C_4H_6O_5S$**
		$C_5H_{10}O_4S$	**$C_5H_{10}O_4S$**
		$C_6H_{14}O_3S$	$C_6H_{14}O_3S$
178	$C_{14}H_{10}$	$C_6H_{10}O_4S$	$C_6H_{10}O_4S$
		$C_5H_6O_5S$	**$C_5H_6O_5S$**
180	$C_9H_8O_4$	$C_{10}H_{12}OS$	**$C_5H_8O_5S$**
			$C_6H_{12}O_2S_2$
			$C_6H_{12}O_4S$

The formula with grey back colour and the bold number were found to be the precursors of organic ambient aerosol with the same molecular compositions.

The bold number were found in ambient atmospheric aerosols with the same molecular compositions

Table S6: Tentative organic sulfur compounds detected in the present study that were identified in ambient atmospheric aerosols

Reaction system	m/z	Tentative chemical formulas	References*
DMSO	152	$C_4H_8O_4S$ [a]	6
	168	$C_5H_{12}O_4S$ [a]	6, 7
	202	$C_7H_6O_5S$ [b]	7
		$C_8H_{10}O_4S$ [c]	6
	(260)	**($C_6H_{12}O_9S$)**	7
	278	**$C_{12}H_{22}O_5S$**	6
	280	**$C_{13}H_{28}O_4S$** [a]	6, 7
	292	**$C_{14}H_{28}O_4S$**	7
	320	**$C_{16}H_{32}O_4S$**	6
PHE/DMSO and PYR/DMSO	**242**	**$C_7H_{14}O_7S$**	6, 7
	(274)	**($C_{14}H_{10}O_4S$)**	6, 7
	364	**$C_{18}H_{36}O_5S$**	7-9
PHE/DMSO	184	$C_5H_{12}O_5S$ [a]	6, 7
		$C_4H_8O_6S$ [a]	6
	192	$C_6H_8O_5S$	7
		$C_7H_{12}O_4S$	6
	194	$C_5H_6O_6S$	6
		$C_6H_{10}O_5S$	6, 7
		$C_7H_{14}O_4S$ [a]	6, 7
	196	$C_5H_8O_6S$	6-8
		$C_6H_{12}O_5S$ [a]	6-8
		$C_7H_{16}O_4S$ [a]	6, 7
	222	$C_5H_2O_8S$	7
		$C_7H_{10}O_6S$	6, 7
		$C_8H_{14}O_5S$	6
		$C_9H_{18}O_4S$ [a]	7, 8
PYR/DMSO	**212**	**$C_6H_{12}O_6S$** [a]	6-8
	232	**$C_8H_8O_6S$**	6, 7
	266	**$C_9H_{14}O_7S$**	6-8
	278	**$C_{11}H_{18}O_6S$**	6
	280	**$C_{10}H_{16}O_7S$** [d]	6-8
	282	**$C_{10}H_{18}O_7S$** [d]	6-8
	284	**$C_9H_{16}O_8S$**	6, 8
	294	**$C_{11}H_{18}O_7S$**	6-8
	296	**$C_{11}H_{20}O_7S$**	6-8

	298	**$C_{16}H_{10}O_4S$**	7
	312	**$C_{11}H_{20}O_8S$**	6-8
	(322)	**($C_{14}H_{26}O_6S$)**	6-9
	324	**$C_{14}H_{28}O_6S$** [a]	6-8
	326	**$C_{12}H_{22}O_8S$**	7
	334	**$C_{16}H_{30}O_5S$**	8, 9
	336	**$C_{14}H_{24}O_7S$**	6, 8
	338	**$C_{13}H_{22}O_8S$**	6-8
	350	**$C_{14}H_{22}O_8S$**	6, 7
	352	**$C_{16}H_{32}O_6S$** [a]	6-8
	354	**$C_{13}H_{22}O_9S$**	6, 7
	366	**$C_{14}H_{22}O_9S$**	6
		$C_{15}H_{26}O_8S$	6
	(380)	**($C_{15}H_{24}O_9S$)**	6
	382	**$C_{15}H_{26}O_9S$**	6, 7
PAHs/DMSO and DMSO	80	CH_4O_2S** (MSIA)	
	94	$C_2H_6O_2S$**(MSM)	
	96	CH_4O_3S**(MSA)	
	112	CH_4O_4S**(MSAOH)	
	126	$C_2H_6O_4S$**(ESAOH)	
	166	$C_4H_6O_5S$	6
		$C_5H_{10}O_4S$ [a]	6, 7
	178	$C_5H_6O_5S$	7
	180	$C_5H_8O_5S$ [e]	6
		$C_6H_{12}O_4S$ [a]	6, 7
PYR/DMSO, PHE/DMSO and DMSO	124	$C_3H_8O_3S$**(EMS)	
		$C_2H_4O_4S$	6
	140	$C_3H_8O_4S$ [a]	6
	154	$C_4H_{10}O_4S$ [a]	6
		$C_3H_6O_5S$ [a, e]	6
	156	$C_2H_4O_6S$ [a, e]	6
	170	$C_3H_6O_6S$ [a, e]	6
		$C_4H_{10}O_5S$ [a]	6
	216	**$C_8H_8O_5S$** [b]	6-8
FLA/DMSO, PHE/DMSO and DMSO	182	$C_4H_6O_6S$	6
		$C_5H_{10}O_5S$ [a, e]	6, 7, 9
		$C_6H_{14}O_4S$ [a]	6, 7
PHE/DMSO and DMSO	204	$C_7H_8O_5S$	7
	206	$C_7H_{10}O_5S$	6, 7
		$C_8H_{14}O_4S$	6
	208	$C_6H_8O_6S$	6, 7
		$C_7H_{12}O_5S$	6

	210	$C_8H_{16}O_4S$ [a]	6, 7, 9
		$C_6H_{10}O_6S$	6, 7
		$C_7H_{14}O_5S$ [a]	6, 7
		$C_8H_{18}O_4S$ [a]	6 7

Chemical formulae in bold were detected in aqueous solutions. Those chemical formulae with brackets were only detected under dark condition.

*References related to the chemical formulae of organic sulfur compounds identified in ambient aerosols.

** Chemical formulae correspond to the organic sulfur compounds, known to participate in the NPF events.

Tentatively identified VOC precursors:

[a] alkyl OS. [b] 2-methylnaphthalene. [c] methylbenzyl sulfate. [d] α,β-Pinene, Limonene, α,β-Terpinene. [e] Isoprene.

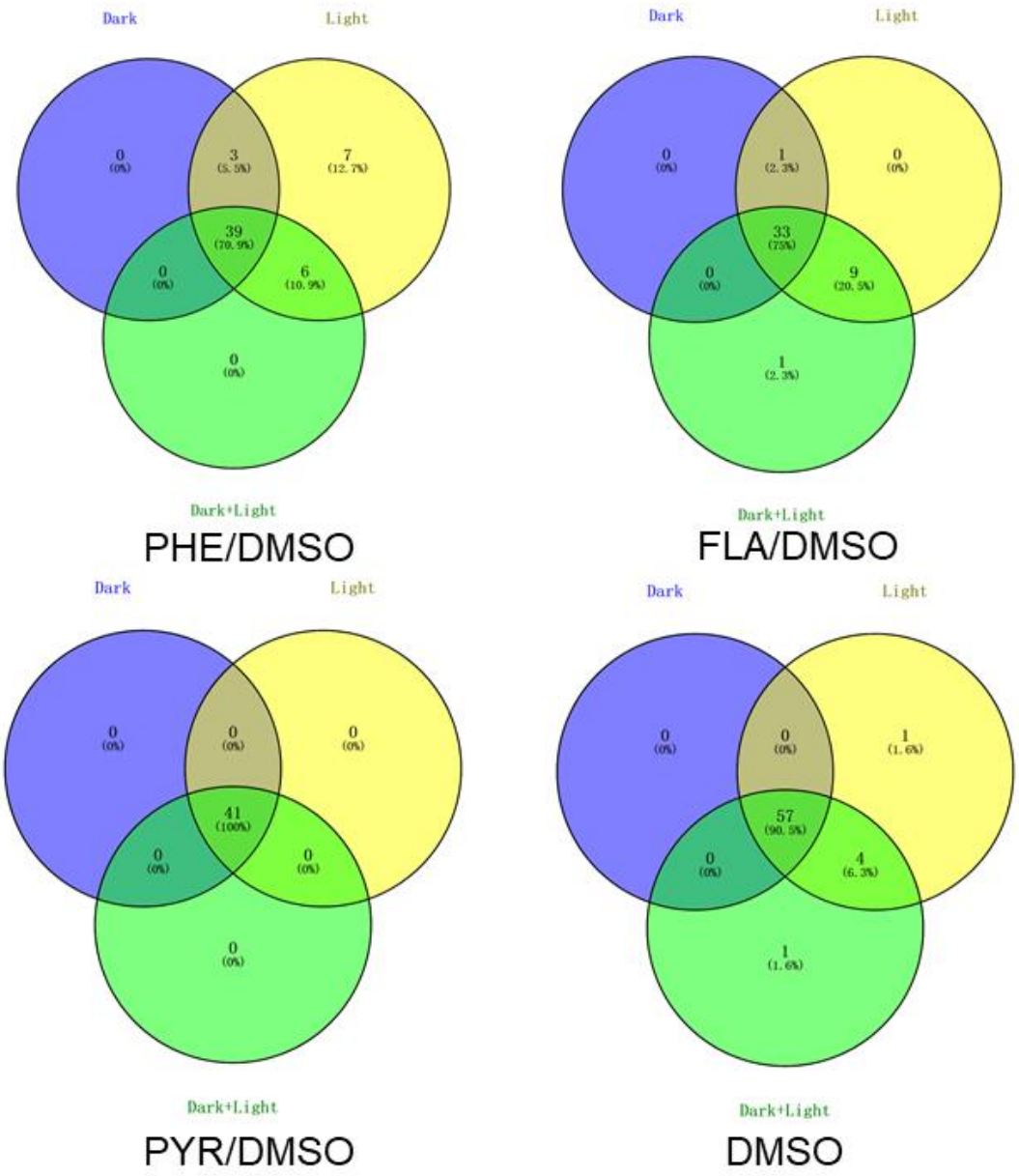

Figure S1: Venn Diagrams of gaseous compounds detected upon reaction of SO_2 with PAHs/DMSO and DMSO.

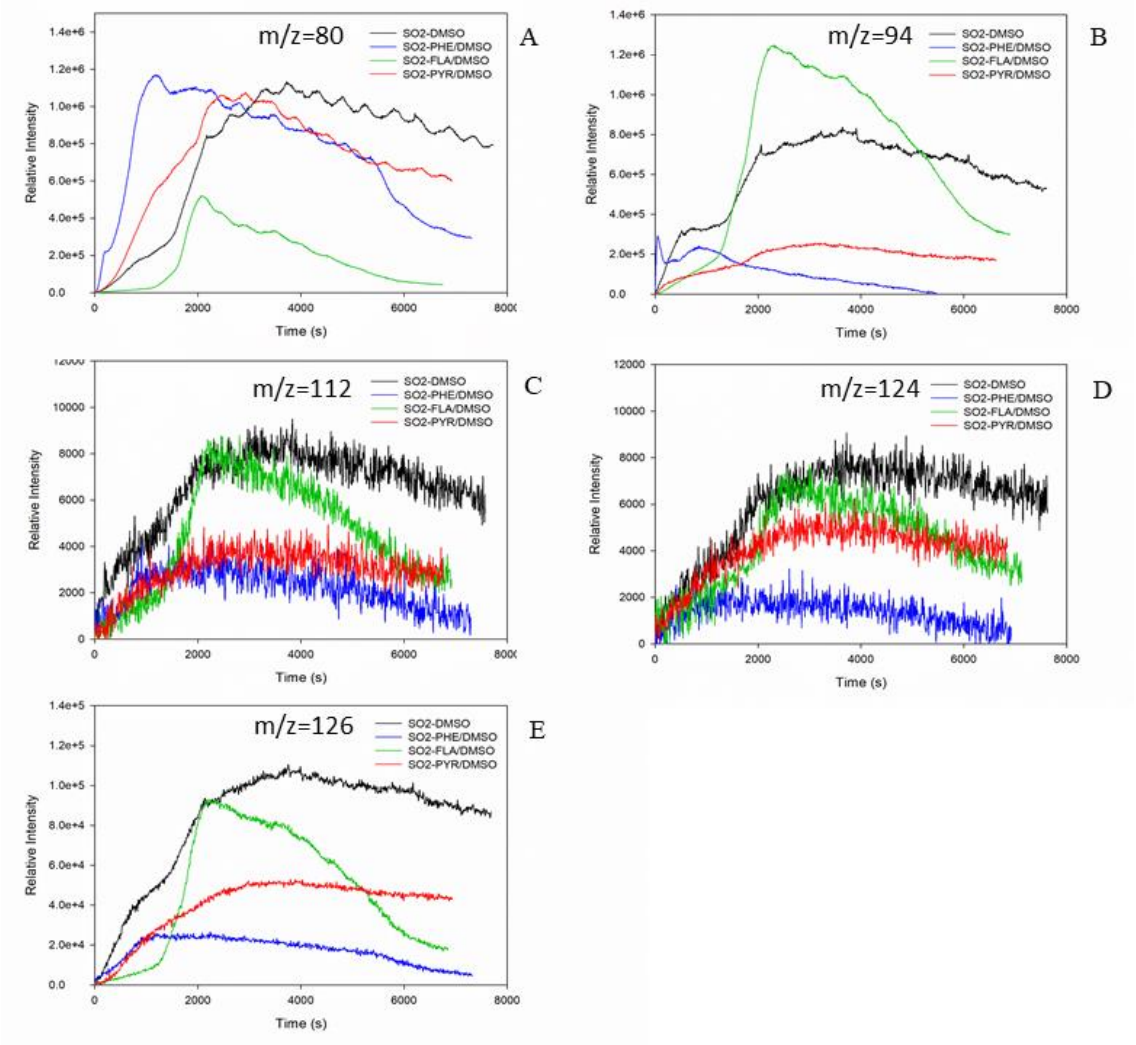

Figure S2: Formation profiles of m/z=80 (MSIA) (Panel A), m/z=94 (MSM) (Panel B), m/z=112 (MSAOH) (Panel C), m/z=124 (EMS) (Panel D) and m/z=126 (ESAOH) (Panel E) upon light-induced heterogeneous reactions of SO_2 with PAHs/DMSO.

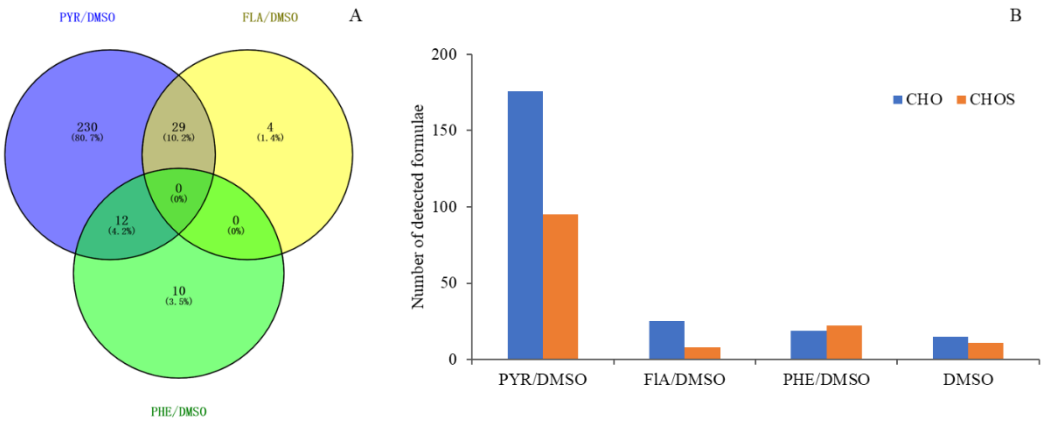

Figure S3: Venn Diagrams of the detected aqueous-phase product compounds formed during the heterogeneous reaction of SO_2 with PAHs/DMSO under light irradiation (300 nm<λ<700nm) (Panel A); Total number of detected formulae for the heterogeneous reactions of SO_2 with DMSO and PAHs/DMSO upon light irradiation (Panel B).

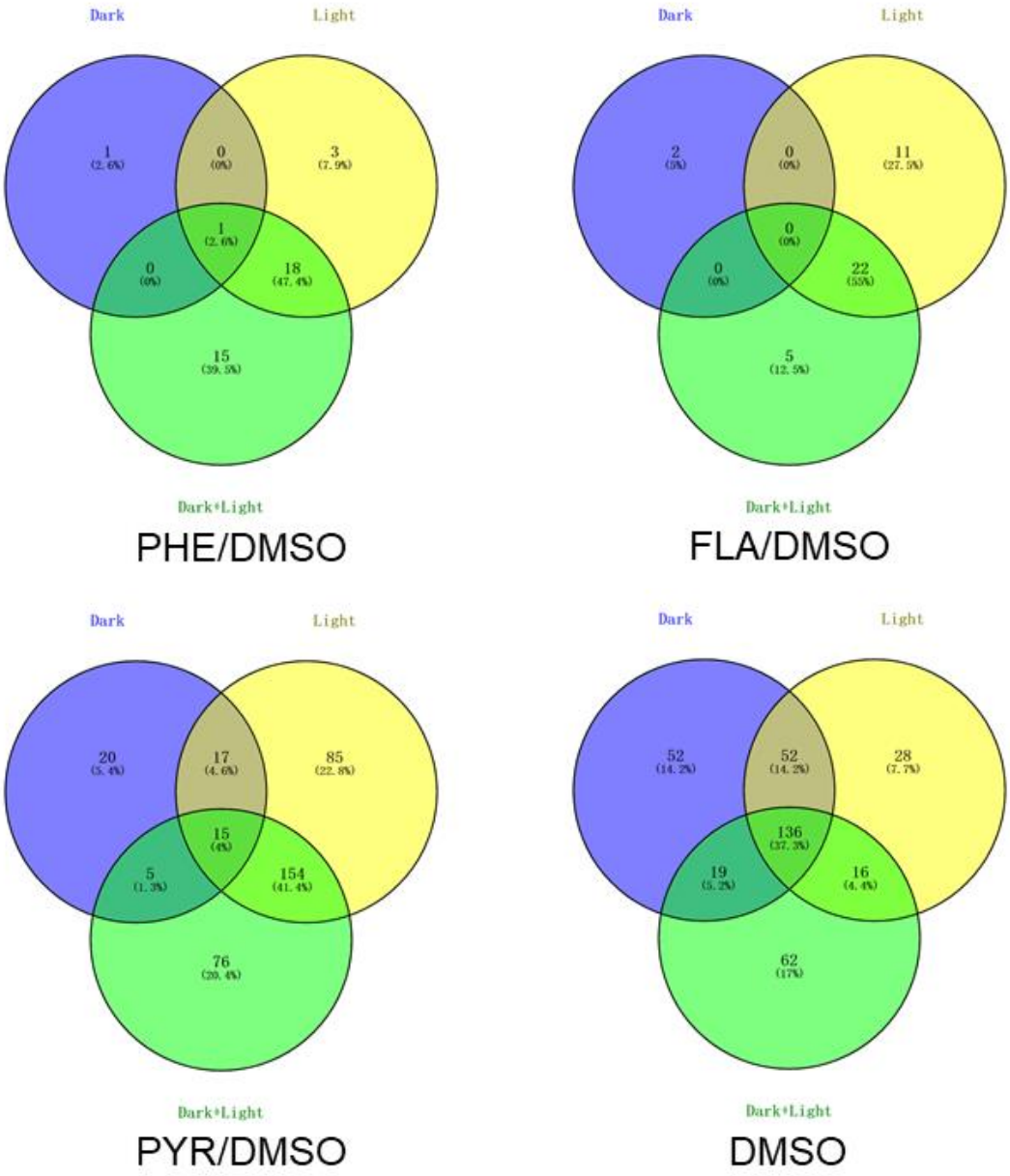

Figure S4: Venn Diagrams of aqueous compounds detected upon reaction of SO_2 with PAHs/DMSO and DMSO.

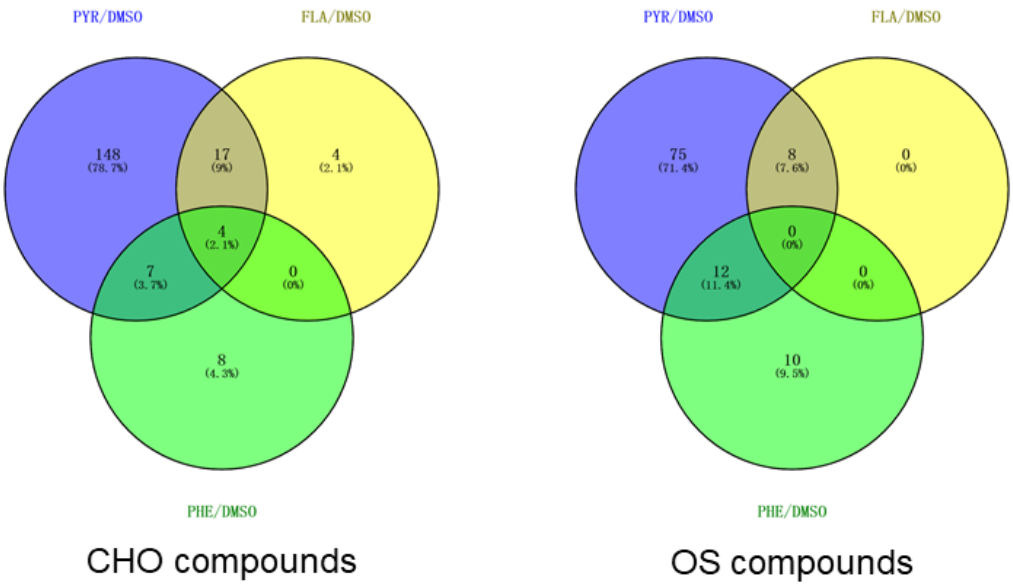

Figure S5: Venn Diagrams of $C_cH_hO_o$ (CHO) and $C_cH_hO_oS_s$ (CHOS) compounds detected upon reaction of SO_2 with PAHs/DMSO and DMSO in the aqueous phase.

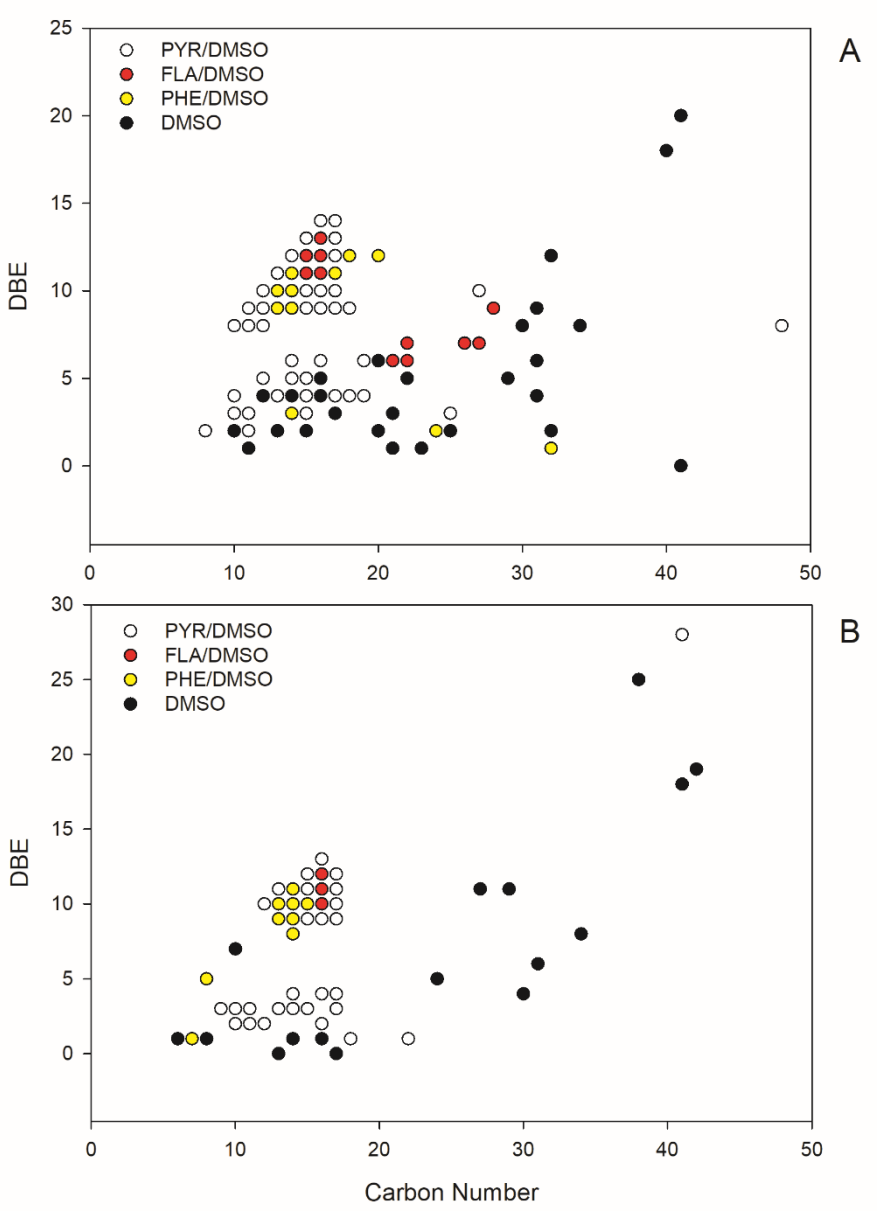

Figure S6: DBE versus carbon number isoabundance plots for the $C_cH_hO_o$ (panel A) and $C_cH_hO_oS_s$ (panel B) group of products detected in ESI^- mode, emerged by the light-induced heterogeneous reaction of SO_2 with PAHs/DMSO.

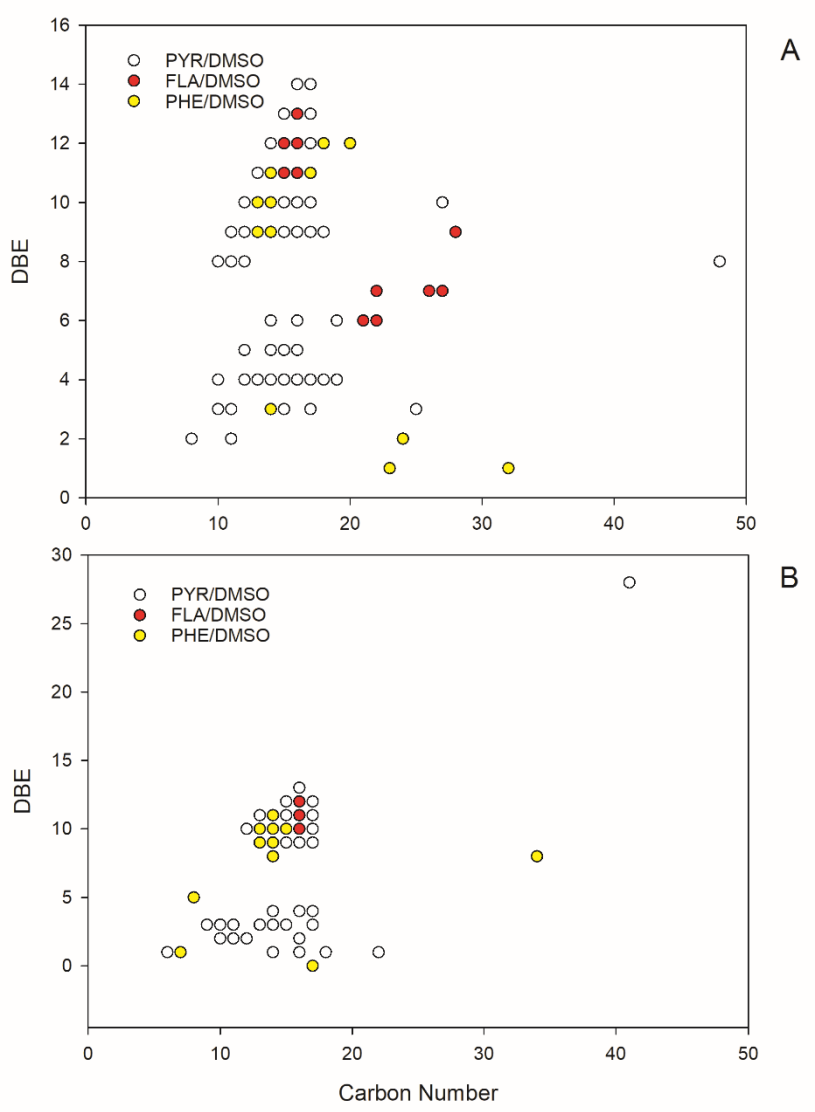

Figure S7: DBE versus carbon number isoabundance plot for the $C_cH_hO_o$ (Panel A) and $C_cH_hO_oS_s$ (Panel B) group of compounds detected in ESI^- mode, emerged by the light-induced heterogeneous reaction of SO_2 with PAHs/DMSO.

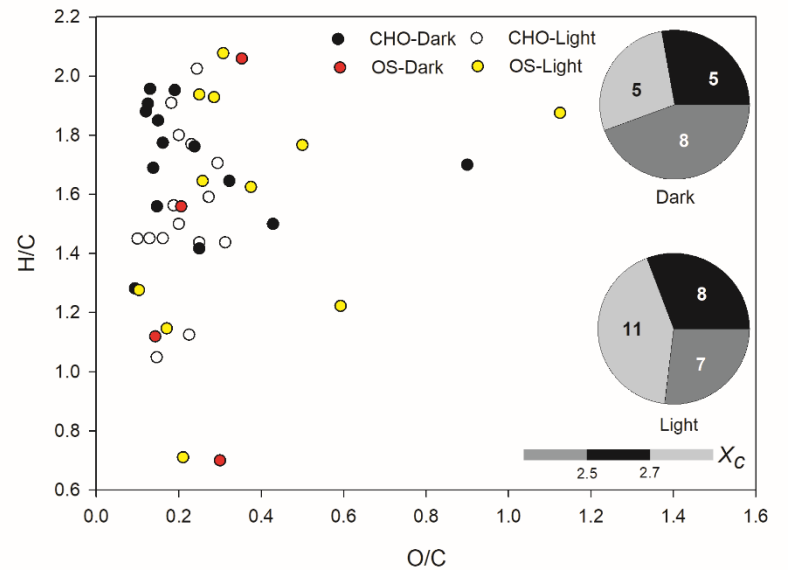

Figure S8: The van Krevelen graph and aromaticity equivalent (grey with X_c < 2.5, black with 2.5 $\leqslant$ X_c < 2.7, and silver with X_c $\geqslant$ 2.7) for detected $C_cH_hO_o$ (CHO) and $C_cH_hO_oS_s$ (CHOS) compounds detected in ESI^- mode, formed by the heterogeneous reactions of SO_2 with DMSO in dark and in presence of light. The X_c is illustrated by the color bar of each VK diagram, while the pie chart demonstrates the number in different thresholds.

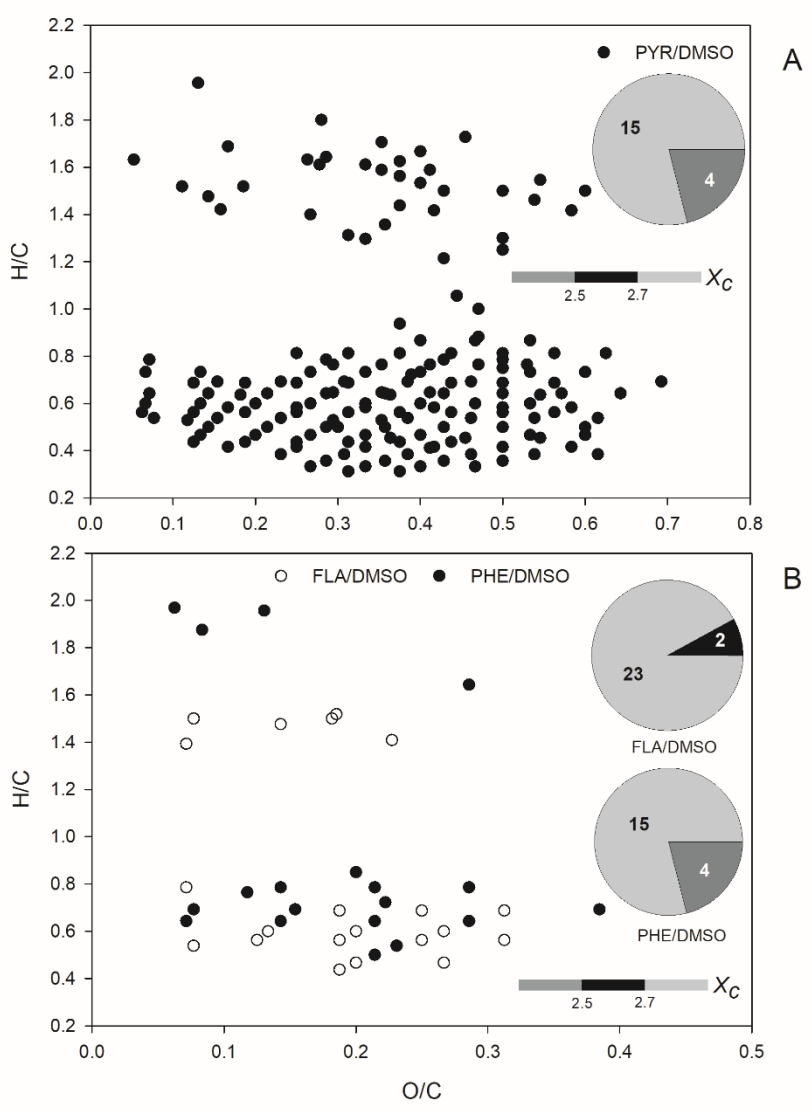

Figure S9: The van Krevelen graph and aromaticity equivalent (grey with X_c < 2.5, black with 2.5 ⩽ X_c < 2.7, and silver with X_c ⩾ 2.7) for detected $C_cH_hO_o$ compounds in ESI^- mode, formed by the heterogeneous reaction of SO_2 with PAHs/DMSO in presence of light. The X_c is illustrated by the color bar of each VK diagram, while the pie chart demonstrates the number in different thresholds during these reactions.

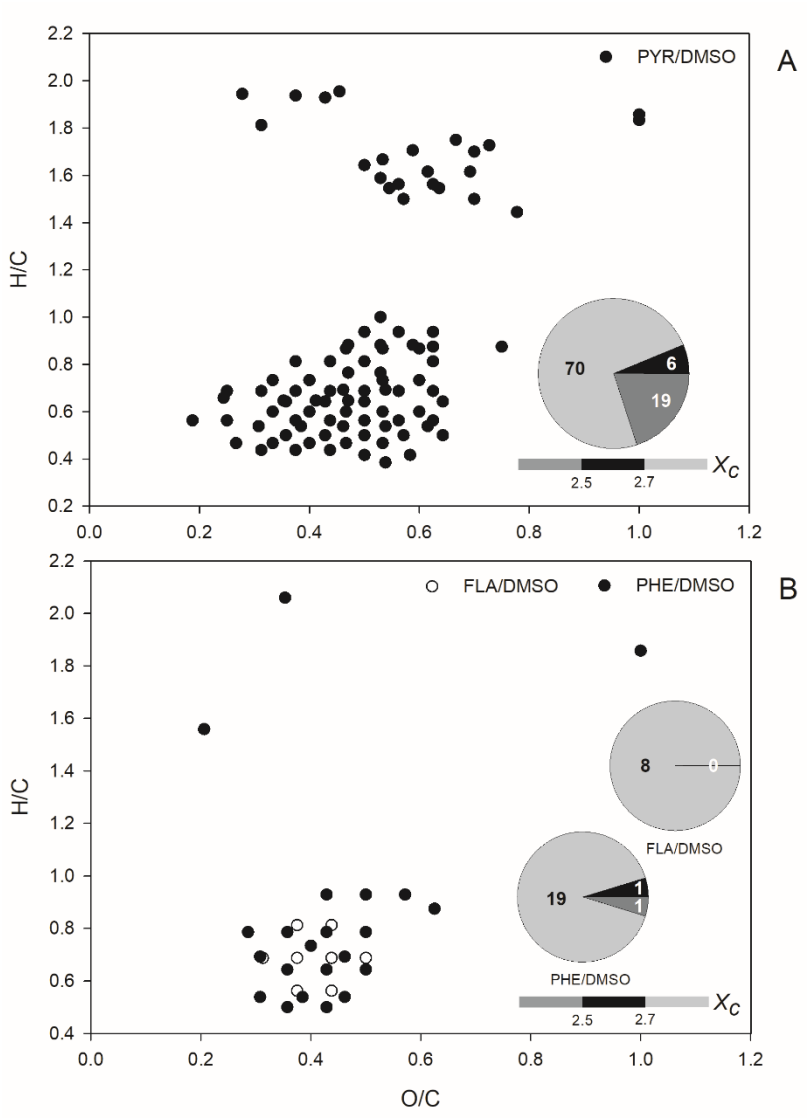

Figure S10: The van Krevelen graph and aromaticity equivalent (grey with X_c < 2.5, black with 2.5 ⩽ X_c < 2.7, and silver with X_c ⩾ 2.7) for detected $C_cH_hO_oS_s$ compounds in ESI^- mode, formed by the heterogeneous reaction of SO_2 with PAHs/DMSO in presence of light. The X_c is illustrated by the color bar of each VK diagram, while the pie chart demonstrates the number in different thresholds during these reactions.

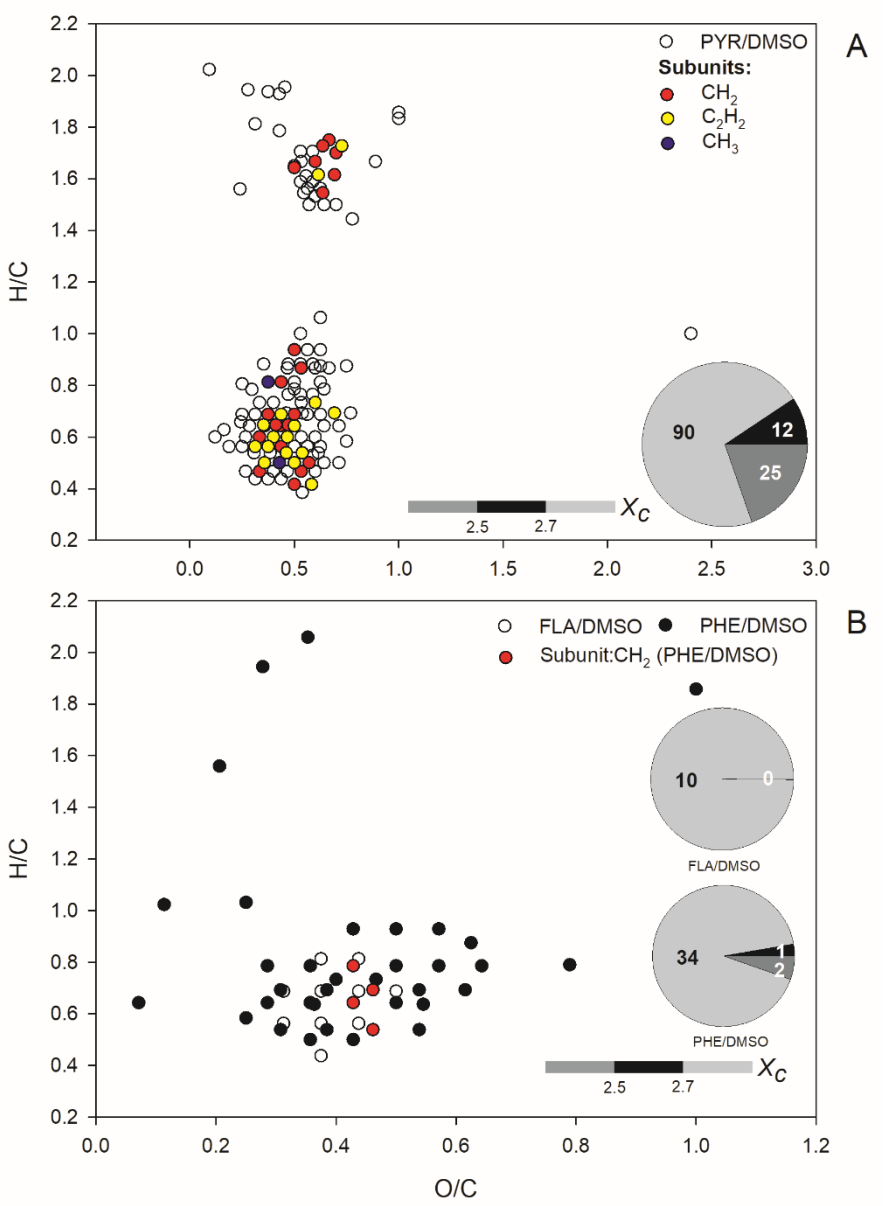

Figure S11: The van Krevelen graph and aromaticity equivalent (grey with X_c < 2.5, black with 2.5 ⩽ X_c < 2.7, and silver with X_c ⩾ 2.7) for detected $C_cH_hO_oS_s$ compounds in ESI^- mode formed during the heterogeneous reaction of SO_2 with PAHs/DMSO upon all experimental conditions. The X_c is illustrated by the color bar of each VK diagram, while the pie chart demonstrates the number in different thresholds during these reactions.

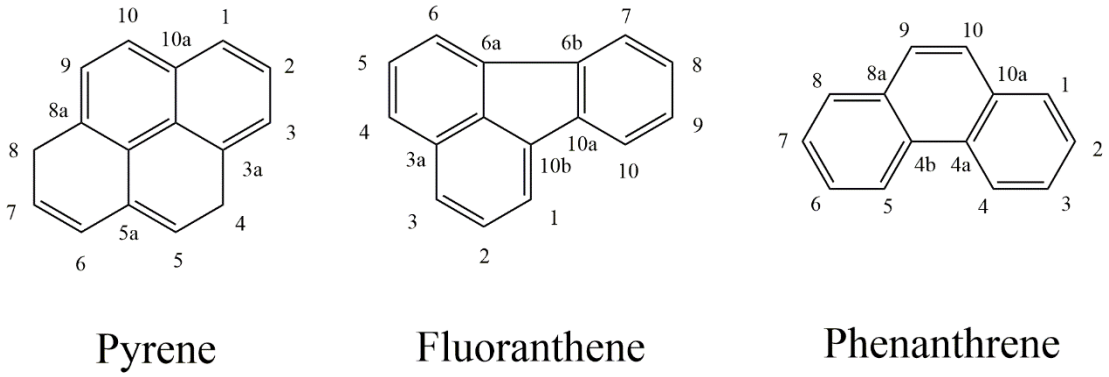

Pyrene Fluoranthene Phenanthrene

Figure S12: Structures of pyrene, fluoranthene and phenanthrene and their numbering convention.

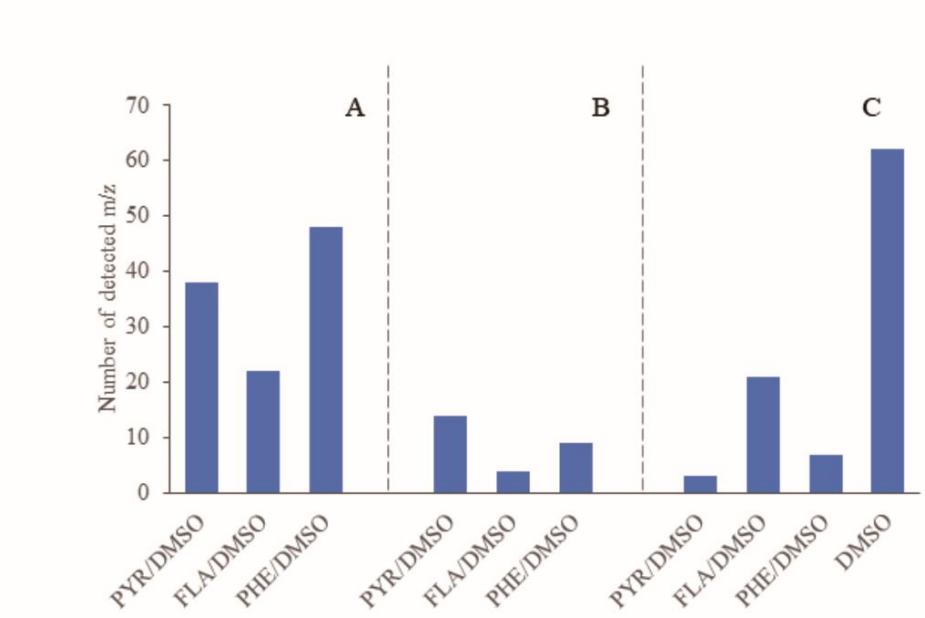

Figure S13: The total number of identified *m/z* signals upon (**A**) both, the photodegradation of PYR/DMSO, FLA/DMSO, and PHE/DMSO and light-induced reaction of SO_2 with DMSO, PYR/DMSO, FLA/DMSO, and PHE/DMSO, (**B**) only photodegradation of PYR/DMSO, FLA/DMSO, and PHE/DMSO and (**C**) only light-induced reaction of SO_2 with DMSO, PYR/DMSO, FLA/DMSO, and PHE/DMSO

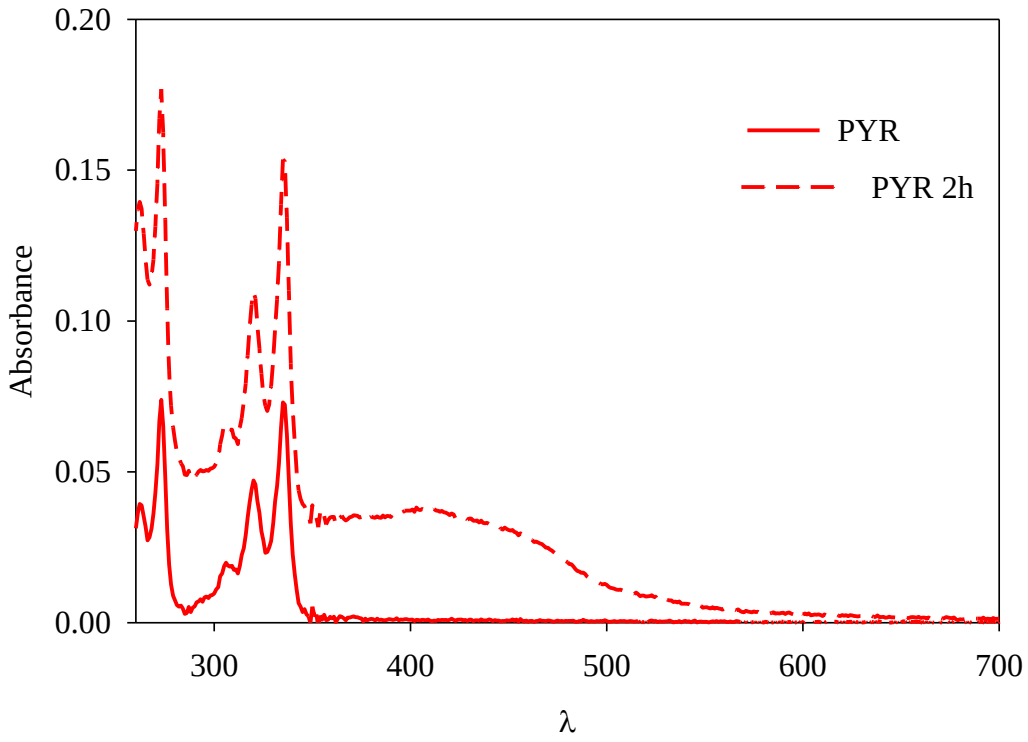

Figure S14: UV-VIS absorption spectra of pyrene/DMSO in the aqueous phase taken before the irradiation and after 2 h of light irradiation

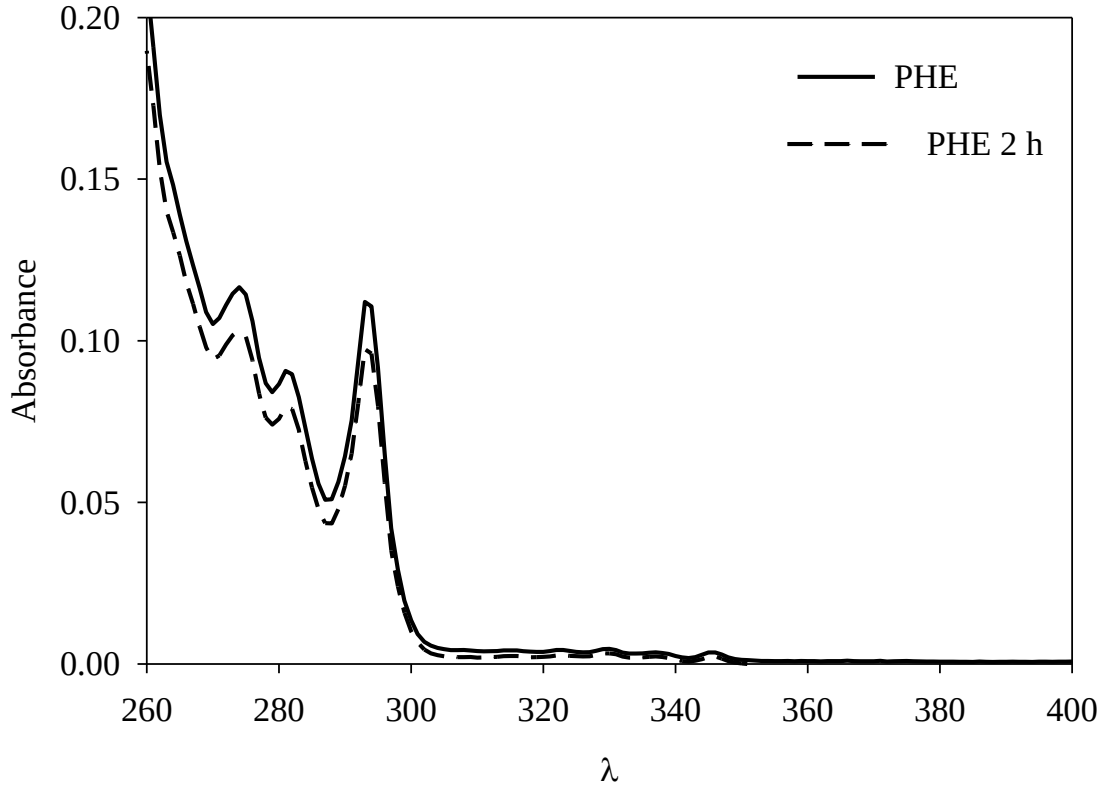

Figure S15: UV-VIS absorption spectra of phenathrene/DMSO in the aqueous phase taken before the irradiation and after 2 h of light irradiation

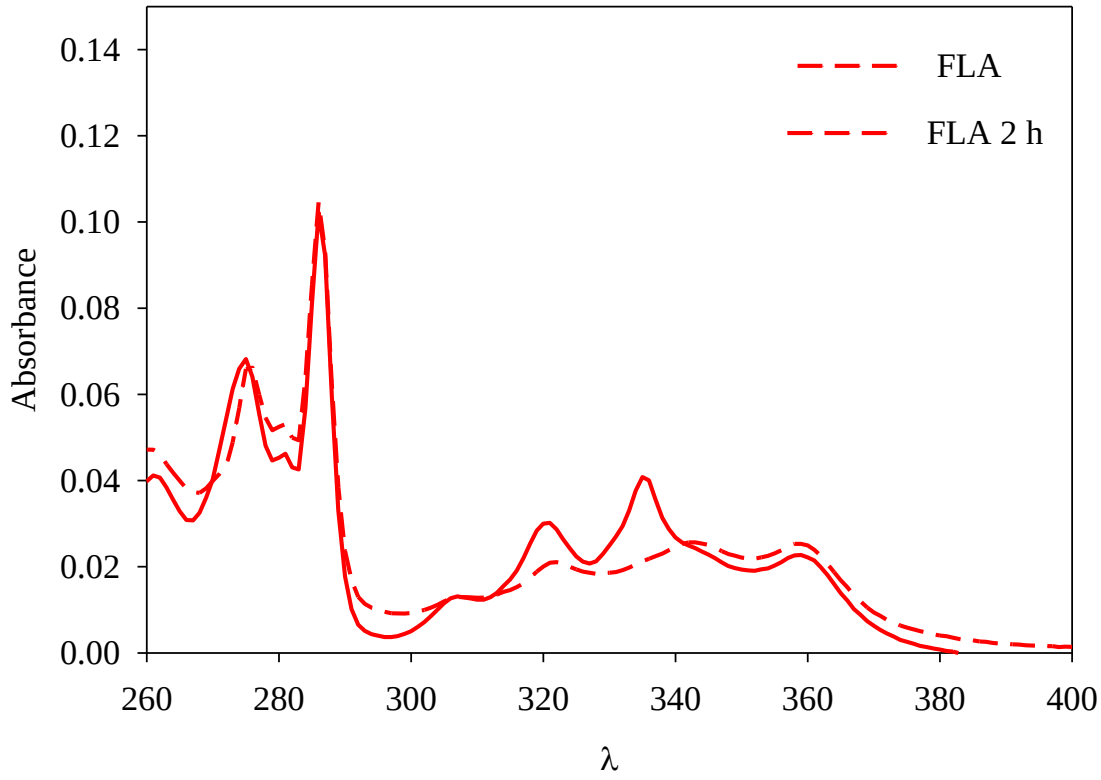

Figure S16: UV-VIS absorption spectra of fluonanthrene/DMSO in the aqueous phase taken before the irradiation and after 2 h of light irradiation

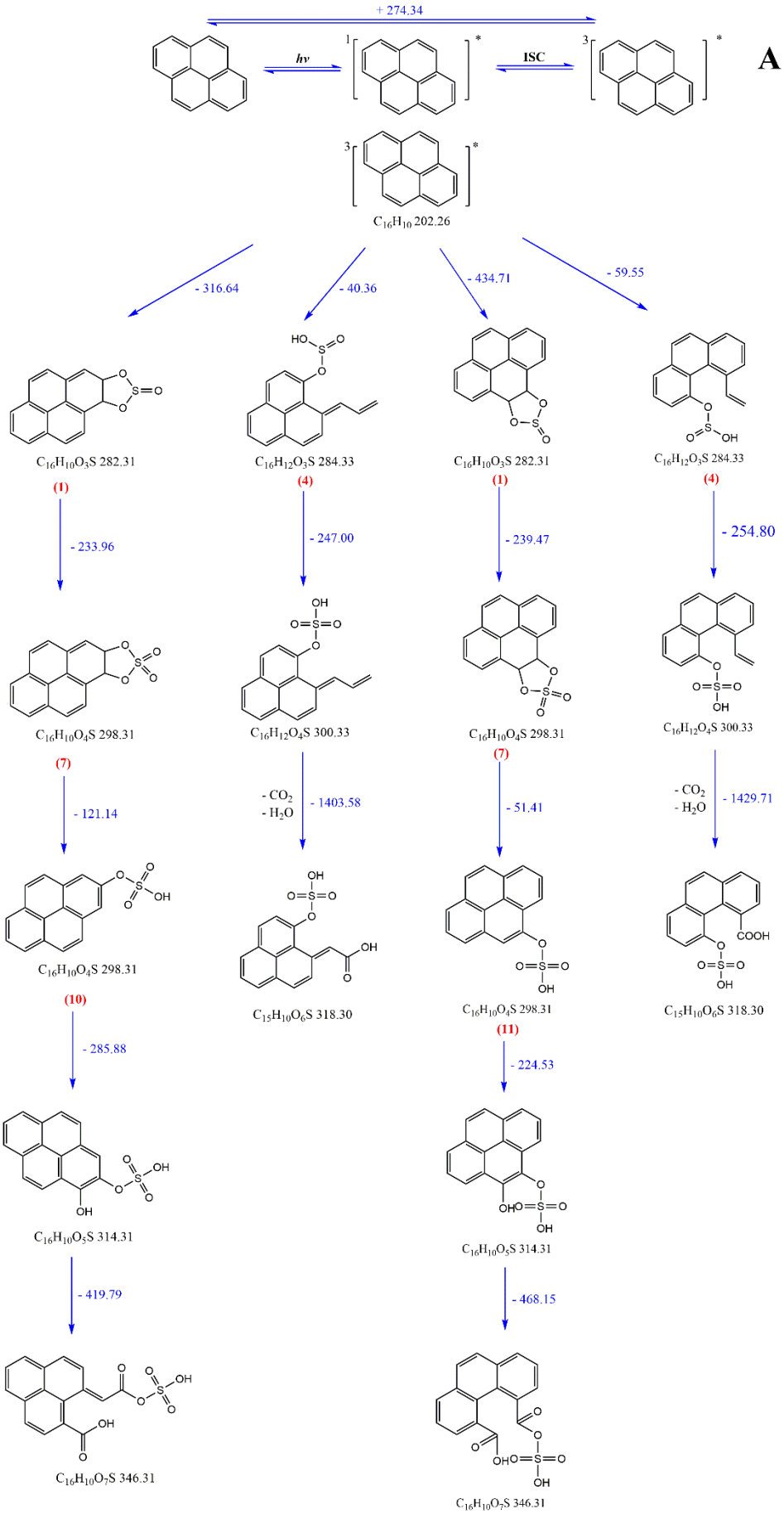
+ 274.34
hv
ISC
A
C16H10 202.26
- 316.64
- 40.36
- 434.71
- 59.55
C16H10O3S 282.31
C16H12O3S 284.33
C16H10O3S 282.31
C16H12O3S 284.33
(1)
(4)
(1)
(4)
- 233.96
- 247.00
- 239.47
- 254.80
C16H10O4S 298.31
C16H12O4S 300.33
C16H10O4S 298.31
C16H12O4S 300.33
(7)
- CO2
- H2O
(7)
- CO2
- H2O
- 121.14
- 1403.58
- 51.41
- 1429.71
C16H10O4S 298.31
C15H10O6S 318.30
C16H10O4S 298.31
C15H10O6S 318.30
(10)
(11)
- 285.88
- 224.53
C16H10O5S 314.31
C16H10O5S 314.31
- 419.79
- 468.15
C16H10O7S 346.31
C16H10O7S 346.31

B

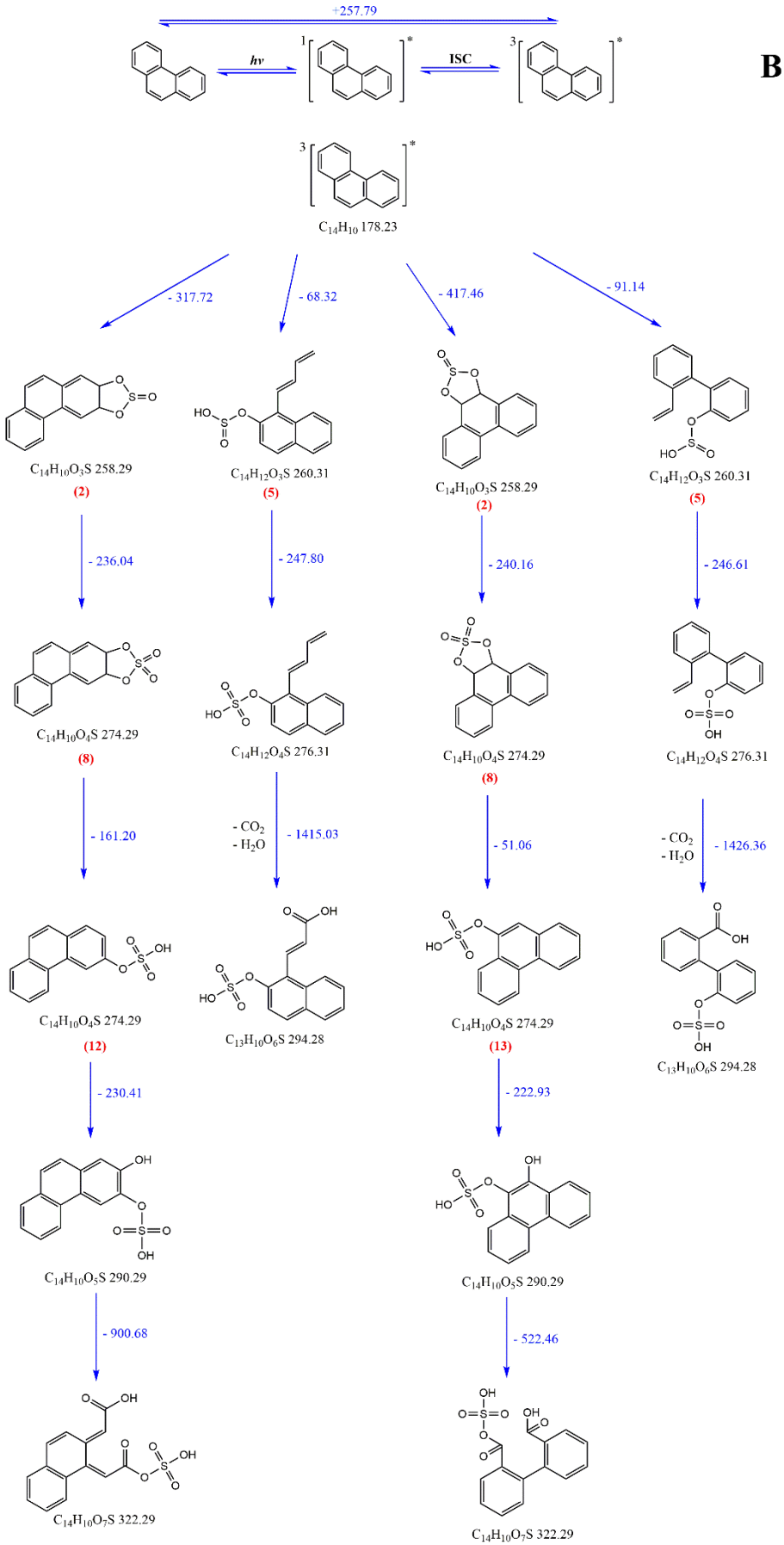
+257.79
hv
ISC
C14H10 178.23
- 317.72
- 68.32
- 417.46
- 91.14
C14H10O3S 258.29
(2)
C14H12O3S 260.31
(5)
C14H10O3S 258.29
(2)
C14H12O3S 260.31
(5)
- 236.04
- 247.80
- 240.16
- 246.61
C14H10O4S 274.29
(8)
C14H12O4S 276.31
C14H10O4S 274.29
(8)
C14H12O4S 276.31
- 161.20
- CO2
- H2O
- 1415.03
- 51.06
- CO2
- H2O
- 1426.36
C14H10O4S 274.29
(12)
C13H10O6S 294.28
C14H10O4S 274.29
(13)
C13H10O6S 294.28
- 230.41
- 222.93
C14H10O5S 290.29
C14H10O5S 290.29
- 900.68
- 522.46
C14H10O7S 322.29
C14H10O7S 322.29

C

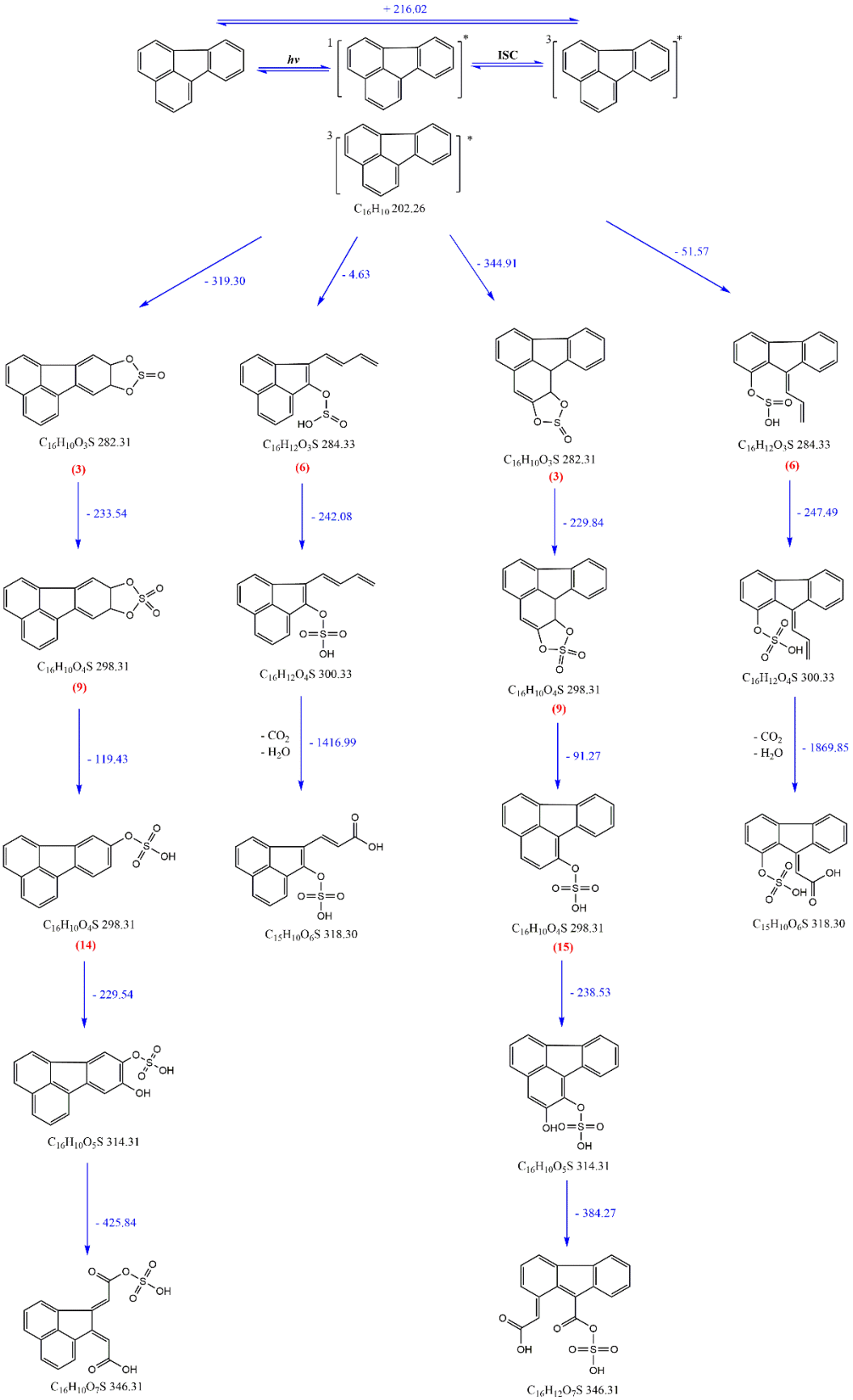
+ 216.02
hv
ISC
C16H10 202.26
- 319.30
- 4.63
- 344.91
- 51.57
C16H10O3S 282.31
(3)
- 233.54
C16H10O4S 298.31
(9)
- 119.43
C16H10O4S 298.31
(14)
- 229.54
C16H10O5S 314.31
- 425.84
C16H10O7S 346.31
C16H12O3S 284.33
(6)
- 242.08
C16H12O4S 300.33
- CO2
- H2O
- 1416.99
C15H10O6S 318.30
C16H10O3S 282.31
(3)
- 229.84
C16H10O4S 298.31
(9)
- 91.27
C16H10O4S 298.31
(15)
- 238.53
C16H10O5S 314.31
- 384.27
C16H12O7S 346.31
C16H12O3S 284.33
(6)
- 247.49
C16H12O4S 300.33
- CO2
- H2O
- 1869.85
C15H10O6S 318.30

Scheme S1: Detailed reaction mechanism describing the OSs formation of aqueous phase products initiated by ^{3}PAHs* and $^{3}SO_2$*. Numbers in brackets, written below each molecule, present compound designations to better follow the discussion with Scheme S1.

References

1. Jiang, B.; Liang, Y.; Xu, C.; Zhang, J.; Hu, M.; Shi, Q., Polycyclic aromatic hydrocarbons (PAHs) in ambient aerosols from Beijing: characterization of low volatile PAHs by positive-ion atmospheric pressure photoionization (APPI) coupled with Fourier transform ion cyclotron resonance. *Environ. Sci. Technol.* **2014,** *48*, (9), 4716-23.

2. Mekic, M.; Liu, J.; Zhou, W.; Loisel, G.; Cai, J.; He, T.; Jiang, B.; Yu, Z.; Lazarou, Y. G.; Li, X.; Brigante, M.; Vione, D.; Gligorovski, S., Formation of highly oxygenated multifunctional compounds from cross-reactions of carbonyl compounds in the atmospheric aqueous phase. *Atmos. Environ.* **2019,** *219*.

3. Vione, D.; Albinet, A.; Barsotti, F.; Mekic, M.; Jiang, B.; Minero, C.; Brigante, M.; Gligorovski, S., Formation of substances with humic-like fluorescence properties, upon photoinduced oligomerization of typical phenolic compounds emitted by biomass burning. *Atmos. Environ.* **2019,** *206*, 197-207.

4. Passananti, M.; Kong, L.; Shang, J.; Dupart, Y.; Perrier, S.; Chen, J.; Donaldson, D. J.; George, C., Organosulfate Formation through the Heterogeneous Reaction of Sulfur Dioxide with Unsaturated Fatty Acids and Long‐Chain Alkenes. *Angew. Chem. Int. Ed.* **2016,** *55*, (35), 10336-10339.

5. Shang, J.; Passananti, M.; Dupart, Y.; Ciuraru, R.; Tinel, L.; Rossignol, S. p.; Perrier, S. b.; Zhu, T.; George, C., SO2 Uptake on oleic acid: A new formation pathway of organosulfur compounds in the atmosphere. *Environ. Sci. Technol. Lett.* **2016,** *3*, (2), 67-72.

6. Kuang, B. Y.; Lin, P.; Hu, M.; Yu, J. Z., Aerosol size distribution characteristics of organosulfates in the Pearl River Delta region, China. *Atmos. Environ.* **2016,** *130*, 23-35.

7. Wang, X. K.; Rossignol, S.; Ma, Y.; Yao, L.; Wang, M. Y.; Chen, J. M.; George, C.; Wang, L., Molecular characterization of atmospheric particulate organosulfates in three megacities at the middle and lower reaches of the Yangtze River. *Atmospheric Chem. Phys.* **2016,** *16*, (4), 2285-2298.

8. Tao, S.; Lu, X.; Levac, N.; Bateman, A. P.; Nguyen, T. B.; Bones, D. L.; Nizkorodov, S. A.; Laskin, J.; Laskin, A.; Yang, X., Molecular characterization of organosulfates in organic aerosols from Shanghai and Los Angeles urban areas by nanospray-desorption electrospray ionization high-resolution mass spectrometry. *Environ. Sci. Technol.* **2014,** *48*, (18), 10993-1001.

9. Zhu, M.; Jiang, B.; Li, S.; Yu, Q.; Yu, X.; Zhang, Y.; Bi, X.; Yu, J.; George, C.; Yu, Z., Organosulfur Compounds Formed from Heterogeneous Reaction between SO2 and Particulate-Bound Unsaturated Fatty Acids in Ambient Air. *Environ. Sci. Technol. Lett.* **2019,** *6*, (6), 318-322.